

# Combined stellar structure and atmosphere models for massive stars

## IV. The impact on the ionization structure of single star H II regions

Grażyna Stasińska<sup>1</sup> and Daniel Schaerer<sup>2</sup>

<sup>1</sup> DAEC, Observatoire de Meudon, 92195 Meudon Cedex, France (grazyna@obspm.fr)

<sup>2</sup> Space Telescope Science Institute, 3700 San Martin Drive, Baltimore, MD 21218, USA (schaerer@stsci.edu)

Received 6 August 1996 / Accepted October 1996

**Abstract.** We study the impact of modern stellar atmospheres that take into account the effects of stellar winds, departures from LTE and line blanketing (“*CoStar*” models) on the ionization structure of H II regions. Results from a large grid of photoionization models are presented. Due to a flatter energy distribution in the He I continuum, compared to the widely used Kurucz models, generally higher ionic ratios are obtained.

We find that N<sup>+</sup>/O<sup>+</sup> and Ne<sup>++</sup>/O<sup>++</sup> can be safely used as direct indicators of N/O and Ne/O abundance ratios in H II regions, over a wide range of astrophysical situations.

The roughly constant observed value of Ne<sup>++</sup>/O<sup>++</sup> ionic ratios in Galactic H II regions is naturally reproduced by photoionization models using *CoStar* fluxes, while Kurucz models at solar metallicity fail to reproduce this behaviour. This gives support to ionizing fluxes from non-LTE atmospheres including stellar winds and line blanketing. However, we also point out that tests of stellar atmosphere models from observations of H II regions are hampered by a lack of strong constraints on the ionization parameter.

**Key words:** H II regions – ISM: abundances – stars: atmospheres – stars: mass-loss – stars: early-type – ultraviolet: stars

### 1. Introduction

Most of the recent work on H II regions modelling uses the Kurucz (1991) plane-parallel LTE model atmospheres. There are two reasons to this. One is that Kurucz’s computations include line blanketing, which is indeed impor-

tant in stellar atmospheres, especially at high metallicities. This effect was not included in earlier non-LTE stellar atmosphere modelling (e.g. Mihalas & Auer 1970). The other reason is that Kurucz models are available for a wide set of stellar temperatures and metallicities, which makes them extremely useful for any study aimed at reproducing the observed properties of H II regions in different environments.

However, it is recognized that Kurucz models cannot predict correctly the distribution of the radiation in the Lyman continuum of hot stars, not only because non-LTE effects are neglected, but also because the presence of winds in such stars is expected to have an impact on the outgoing stellar flux (Gabler et al. 1989, Najarro et al. 1996, Schaerer et al. 1996b).

A new set of theoretical stellar spectra from the combined stellar structure and atmosphere models (referred to as *CoStar* models) of Schaerer et al. (1996a, b) has now been published (Schaerer & de Koter 1996, hereafter SdK96). The atmosphere, in particular, includes the effects of stellar winds, departure from LTE as well as blanketing. It is the purpose of this paper to explore the impact of these new ionizing fluxes on single star H II region models.

In Section 2, we recall the main features of the *CoStar* models, and discuss the expected uncertainties. In Section 3, we present a grid of photoionization models constructed for metallicities solar ( $Z\odot$ ) and one tenth solar ( $Z\odot/10$ ), using the *CoStar* models and the Kurucz ones, and discuss the main differences. In Section 4, we present some implications on H II regions diagnostics. The possibility of testing these new stellar atmosphere models using observations of H II regions is discussed in Sect. 5. Section 6 summarizes the main conclusions of this study.

## 2. Comparison of *CoStar* and Kurucz model atmospheres

### 2.1. Comparison of ionizing fluxes

A detailed comparison of the ionizing fluxes from *CoStar* models with the plane parallel LTE models of Kurucz and also recent non-LTE models of Kunze et al. (1992) and Kunze (1994) is given in SdK96. Here we shall only briefly recall the most important differences between the *CoStar* and the Kurucz fluxes used in our study. Wind models similar to ours have also been presented by Sellmaier et al. (1996).

As an illustration we show in Fig. 1 a comparison between the *CoStar* and Kurucz model fluxes for two dwarf models with  $T_\star \simeq 46000$  and 35000 K respectively. Also indicated are the positions of some ionization potentials relevant to the discussion in forthcoming sections. For the *CoStar* model we plot the continuous spectral energy distribution with the spectral resolution used in the non-LTE calculation. Blanketing due to numerous spectral lines of all elements up to zinc is included in these models by means of an opacity sampling technique (using 20 Å bins) as described in Schaerer & Schmutz (1994). The ionization edges of metals (mostly CNO, Ne, and Ar) found in other models (e.g. Kunze et al. 1992, Kunze 1994) are not treated in our models. On the other hand these may be overestimated if iron peak elements causing an important fraction of metal line blanketing are not included. We note that the recent models of Sellmaier et al. (1996) also lack of pronounced metal ionization edges in the EUV, which seems to confirm our calculations. As discussed in SdK96, a more detailed analysis of this question will be possible with the inclusion of additional metals in the full non-LTE calculations (see e.g. de Koter et al. 1994, 1996).

The largest differences between the Kurucz and *CoStar* models appear in the He II continuum above 54 eV: due to the velocity gradient in the stellar wind a strong non-LTE effect depopulates the He II groundstate and leads to a decrease of the bound-free opacity above 54 eV (cf. Gabler et al. 1989). This explains the larger flux in the He II continuum in non-LTE models accounting for stellar winds (*CoStar*) compared to the Kurucz models. Of more importance for the present study is the flux distribution at lower energies, where the ionization potentials of the most important elements observed in H II regions are located. The essential characteristics of the *CoStar* spectrum in the He I continuum ( $24.6 \text{ eV} < E < 54 \text{ eV}$ ) are (cf. SdK96): 1) a flatter spectral energy distribution, and 2) an increase of the total flux. The flattening of the spectrum mainly results from a wind effect whose strength decreases towards higher energies, since the continuum is formed at larger optical depths. In the considered temperature range non-LTE effects increase the total He I ionizing flux in both plane parallel models and those accounting for stellar winds.

### 2.2. Adopted *CoStar* and Kurucz models

The *CoStar* models are available for two sets of abundances: Solar ( $Z=0.020$  in the notation of SdK96) and low metallicity ( $Z=0.004$ ). We will compare these models with the Kurucz ones at solar and one tenth solar metallicity, which is the closest possible correspondence in metallicity.

In the following, we will compare *CoStar* model atmospheres for main sequence stars (the ones labeled A2–F2 in SdK96) with the available Kurucz models having the closest effective temperature and gravity. We will also consider *CoStar* models for giant stars (the ones labeled A4–D4 in SdK96).

The *CoStar* models provide not only the spectral distribution of the ionizing radiation, but also the stellar radii. The radii of stars modelled with the Kurucz atmospheres are obtained from the calibration of Vacca et al. (1996) for stars of luminosity class V and Ia, for main sequence and giants respectively.

## 3. Photoionization models

### 3.1. Definition of the grid

The photoionization models are constructed with the code PHOTO, the latest description of which can be found in Stasińska & Leitherer (1996, hereafter SL96). A model computed with this version of PHOTO that can be directly compared with the results obtained with other photoionization codes (presented at the Lexington workshop, Ferland et al. 1995) is also given in SL96<sup>1</sup>.

The ionization structure of a nebula is mainly determined by the ionizing radiation field and by the nebular geometry. In the simple case of a sphere of constant gas density  $n$  and constant filling factor  $\epsilon$ , the ionization structure of the heavy elements — for a given spectral distribution of the ionizing radiation field — is essentially a function of the ionization parameter  $U = Q_H/(4\pi R^2 n c)$ , where  $Q_H$  is the number of stellar photons emitted per second above 13.6 eV,  $R$  is the external radius, and  $c$  is the speed of light. It can easily be shown that any combination of  $Q_H$ ,  $n$  and  $\epsilon$  that keeps  $Q_H n \epsilon^2$  constant results in a similar ionization structure. For each star, we have thus computed a series of 4 models of hydrogen density  $n = 10 \text{ cm}^{-3}$  and  $\epsilon=1$ , in which the total stellar luminosity has been multiplied by a factor  $10^6$ ,  $10^3$ , 1,  $10^{-3}$  respectively for the models numbered from 1 to 4. Doing this, one covers the entire range of expected ionization

<sup>1</sup> Extensive results (intensities of about 100 lines in the optical, UV and IR domains, mean ionic fractions and averaged electron temperatures) for the photoionization models computed for this study are accessible by anonymous ftp on ftp.obspm.fr in the directory /pub/obs/grazyna/SS96 and most of them can be found as well on the CD-ROM accompanying the paper “A Database for Galaxy Evolution Modeling”, by Leitherer et al. (1996).

parameters, from the most compact H II regions (number 1) to the most diluted interstellar medium (number 4). Numbers 2–3 correspond roughly to the range of ionization parameters encountered in giant H II regions as found in SL96. The ionization structure of model number 2 is the same as that of a model with a single ionizing star and a gas density of  $n = 10^4 \text{ cm}^{-3}$ . From now on, models number 2 will be called the “reference models”<sup>2</sup>.

Within the range of chemical compositions expected in H II regions, the ionization structure of a nebula is only little dependent of its actual chemical composition.

In building our grid, the chemical composition of the gas was taken solar ( $\text{O/H} = 8.51 \cdot 10^{-4}$  with the abundances of the remaining elements as in SL96) when dealing with solar metallicity stellar atmospheres, and one tenth solar ( $\text{O/H} = 8.51 \cdot 10^{-5}$ ) when dealing with low metallicity atmospheres.

### 3.2. Comparison of photoionization models using CoStar and Kurucz fluxes

The comparison is made in a series of diagrams showing ratios of ionic fractions  $x(\text{X}^{+n})/x(\text{Y}^{+m})$  as a function of the stellar effective temperature  $T_\star$ <sup>3</sup>. Figures 2 and 3 represent the solar abundance models using the *CoStar* fluxes and the Kurucz atmospheres respectively. Figures 4 and 5 are equivalent to Figs. 2 and 3 respectively, but for the low metallicity models. In each figure, the “reference models” with different  $T_\star$  are connected with a thick continuous line for main sequence stars, and a thick dotted line for giants. For each star, models with different values of  $U$  are connected with a thin dotted line.

In Figures 2 – 5 panels a – c give examples of ratios of ionic fractions that are supposed to indicate the stellar effective temperature (e.g. Rubin et al. 1995). Panel a shows  $x(\text{He}^+)/x(\text{H}^+)$ , which depends on the ratio of stellar photons above 24.6 eV and 13.6 eV. Panel b shows  $x(\text{N}^{++})/x(\text{N}^+)$ , and Panel c shows  $x(\text{S}^{+++})/x(\text{S}^{++})$  for the solar abundance models and  $x(\text{Ar}^{+++})/x(\text{Ar}^{++})$  for the low metallicity ones. While the  $x(\text{He}^+)/x(\text{H}^+)$  is accessible from optical and radio measurements of H II regions (assuming a canonical helium abundance),

<sup>2</sup> Actually, a sphere may not be the best approximation to the geometry of H II regions. Therefore, we have also introduced a parameter  $f$ , which is the internal radius of the nebula, in units of the Strömgren radius for a full sphere at an electron temperature of 10000 K. We have computed series of models with  $f = 10^{-2}$  and  $f = 3$ . In the latter case, which is close to a plane parallel model, the average “excitation”, as measured for example by  $[\text{O III}]/[\text{O II}]$  tends to be lower than for a full sphere of the same  $U$  (i.e. with  $Q_H$ ,  $n$ ,  $f$  and  $\epsilon$  combining into the same value of  $Q_H n \epsilon^2 (1 + f^3)^{-2}$ ). This effect is especially important for low effective temperature stars. In this paper, we present only results for  $f = 10^{-2}$ , but the interested reader will find the  $f = 3$  models on the anonymous ftp account.

<sup>3</sup>  $x(\text{X}^{+n})$  is defined as:  $\int n(\text{X}^{+n}) n_e dV / \int n(\text{X}) n_e dV$

$x(\text{N}^{++})/x(\text{N}^+)$  and  $x(\text{S}^{+++})/x(\text{S}^{++})$  are accessible from infra-red measurements.  $x(\text{Ar}^{+++})/x(\text{Ar}^{++})$  can be obtained from optical lines, but only when the electron temperature is sufficiently high for the lines to be measurable, that is to say only at low metallicities. Other ratios involving two subsequent ionization stages of the same element that can be compared in the same way with the observations are  $x(\text{O}^{++})/x(\text{O}^+)$ ,  $x(\text{Ne}^{++})/x(\text{Ne}^+)$ , or  $x(\text{S}^{++})/x(\text{S}^+)$ .

The fact that at a given  $T_\star$ , the *CoStar* models have higher fluxes in the  $\sim 30$  eV – 54 eV region translates into higher ionic ratios in photoionization models computed with *CoStar*, as can be seen in Panels a – c of Figs. 2 – 5. This is conspicuous in ratios involving ions of high ionization potential like  $\text{S}^{++}$  (34.83 eV) or  $\text{Ar}^{++}$  (40.74 eV). On the other hand, the effect is actually marginal on the  $x(\text{He}^+)/x(\text{H}^+)$  ratio for main sequence stars, being noticeable only at effective temperatures smaller than  $\sim 40000$  K. The reason is that, at higher temperatures, there are enough photons above 24.6 eV to fully ionize helium, so that  $x(\text{He}^+)/x(\text{H}^+)$  becomes independent of the model atmosphere.

An effective temperature determined from an ionic ratio such as the ones mentioned above (assuming that one has some idea of the ionization parameter) would thus be *lower* using the *CoStar* models than using the Kurucz models. Note that a similar trend was found by Rubin et al. (1995) when they compared photoionization models constructed using the non-LTE atmospheres of Kunze (1994) rather than the Kurucz ones. If indeed one were to use nebular models to determine the effective temperature, one would of course also have to take care that the volume sampled by the observations are comparable to the volume over which the mean ionic fractions are computed in the models. Furthermore one should also remember that the atomic data used in the photoionization model computations are still incomplete: dielectronic recombination is generally an important process in the ionization balance, but the coefficients for ions of sulfur and argon are not available. Also, charge-transfer reaction rates are only approximately known for many ions. In spite of these difficulties, it may be worthwhile noting that *CoStar* models predict a detectable [Ar IV] 4740 line in a wider range of effective temperatures than the Kurucz models.

Another important issue is that with *CoStar* we have appropriate models for all the evolutionary stages of massive stars. Models for giants tend to produce a higher excitation of the surrounding H II regions than what is expected from extrapolating the dwarf models towards lower effective temperatures. This is clearly seen in Figs. 2 and 4 where the curves representing the giants conspicuously depart from the curves corresponding to main sequence stars. The giant model with  $T_\star \approx 32000$  K is a very strong case, where wind effects flatten the spectrum in the 20 – 40 eV range (cf. SdK96). When using the available Kurucz models, the only difference between giants and main se-

quence stars is in the total luminosity, which induces only a negligible variation in the excitation of the surrounding nebulae, through an increase of the ionization parameter  $U$ .

#### 4. Some consequences for abundance determinations in H II regions

Empirical abundance determinations in H II regions generally use an ionization correction factor scheme first proposed by Peimbert & Costero (1969) based on the similarity of ionization potentials of several ions. For example, to derive the N/O ratio, one generally assumes that  $N/O = N^+/O^+$ , and to derive the Ne/O ratio, one assumes that  $Ne/O = Ne^{++}/O^{++}$ . Actually, photoionization models do not always agree with these empirical schemes (e.g. Rubin 1985, Stasińska 1990). This is not surprising, since the ionization potentials of  $O^+$  and  $N^+$  or  $Ne^+$  are not exactly the same, and the various recombination processes do not have the same strength for these ions. Rubin et al. (1988) have strongly questioned the N/O ratios derived from optical measurements of H II regions (partly because of the implied ionization correction scheme), and they consider the N/O ratios derived from far infrared line measurements assuming  $N/O = N^{++}/O^{++}$  to be far more reliable.

Panels d and e in Figs. 2 – 5 show  $x(N^+)/x(O^+)$  and  $x(N^{++})/x(O^{++})$  respectively as a function of  $T_\star$ . We see that, actually, our models show the  $N^+/O^+$  to be an excellent approximation for N/O in all the range of effective temperatures considered, except for the Kurucz models at solar metallicity. In this case, the slope of the stellar spectrum around 30 eV is much larger than for the other models, inducing a differential effect between  $N^+$  and  $O^+$ . Thus, if *CoStar* models describe the stellar radiation field more accurately than the Kurucz ones, the widely used empirical  $N/O = N^+/O^+$  scheme remains a quite safe approximation. Determining the N/O ratio using  $N^{++}/O^{++}$ , on the other hand, gives rise to important biases since, at high effective temperatures,  $N^{++}$  partly transforms into  $N^{+++}$  and at low effective temperature (when actually  $N^+$  and  $O^+$  are the dominant ionic species), the predicted  $x(N^{++})/x(O^{++})$  becomes much larger than unity.

Panel f in Figs. 2 – 5 plots  $x(Ne^{++})/x(O^{++})$  as a function of  $T_\star$ . We see that, in all the “reference models”, this ratio decreases with decreasing effective temperature, whether one uses the *CoStar* atmospheres or the Kurucz ones. However, the range in  $T_\star$  where  $x(Ne^{++})/x(O^{++})$  is close to unity is much larger when using the *CoStar* atmospheres, because they have flatter spectral energy distributions in the 30 – 40 eV range than the Kurucz ones (see also next Section). Thus, if *CoStar* predicts correctly the stellar energy distribution in the Lyman continuum, one expects the  $Ne^{++}/O^{++}$  to give directly the Ne/O ratios over a wide range of parameter space relevant to H II regions.

#### 5. Possible observational tests of stellar atmosphere models using H II regions

Since the predictions on the ionization structure of H II regions depend so strongly on the type of model atmosphere, one might hope to use observations of H II regions to test the flux of these models in the Lyman continuum.

Along this line, it has already been noted that the so-called [Ne III] problem, which appeared when using the Kurucz model atmospheres, seemed resolved when using model atmospheres, which, similar to *CoStar* models, account for stellar winds, and include a detailed non-LTE treatment and line blocking (Sellmaier et al. 1996, hereafter SYPR96). This [Ne III] problem was made especially clear when Simpson et al. (1995; cf. references therein) obtained far infrared line measurements for a sample of H II regions and plotted the values of  $Ne^{++}/O^{++}$  as a function of  $O^{++}/S^{++}$ . They noted that the observations indicated an essentially flat  $Ne^{++}/O^{++}$  in contradiction with the predictions of photoionization models using the Kurucz atmospheres (assuming no systematic variation in Ne/O or S/O).

In Figures 6 – 9, we show the predictions of our model HII regions for  $Ne^{++}/O^{++}$  to be compared directly to observations. Figures 6 and 7 represent the solar abundance models using the *CoStar* fluxes and the Kurucz atmospheres respectively. Figures 8 and 9 are equivalent to Figs. 6 and 7 respectively, but for the low metallicity models. The layout of the figures is similar to the one used in Figs. 2 – 5. Panel a plots  $Ne^{++}/O^{++} = Ne/O \cdot x(Ne^{++})/x(O^{++})$  as a function of  $O^{++}/S^{++} = O/S \cdot x(O^{++})/x(S^{++})$ . Here, Ne/O and O/S are the standard abundance ratios used by Simpson et al. (1995) ( $Ne/O=0.2$  and  $O/S=47$ ). In Figure 10, we plot the values of  $Ne^{++}/O^{++}$  versus  $O^{++}/S^{++}$  derived from infrared line ratios for the HII regions observed by Simpson et al. (1995), using the atomic data referenced in SL96, and discarding measurements with upper limits only. Our models using *CoStar* have a similar behaviour to the ones of SYPR96), and are in much better agreement with the observations than models based on Kurucz atmospheres. Actually, for the hottest stars, we obtain slightly larger values of  $x(O^{++})/x(S^{++})$  at a given temperature  $T_\star$  than SYPR96. Indeed, the *CoStar* atmospheres seem to produce somewhat higher fluxes in the 40 – 54 eV energy range than the atmospheres of SYPR96. Detailed comparisons will be undertaken to understand the origin of these differences. It appears, however, difficult to distinguish between both cases from nebular observations.

Of course, one should bear in mind that different photoionization codes may produce slightly different ionization structures. A direct comparison can be made for the models using the Kurucz atmospheres. Our computations using PHOTON seem roughly in agreement with the ones of SYPR96, as can be judged by comparing our Fig. 7

with their Fig. 2, and are slightly different from the ones presented in Simpson et al. (1995).

One can also perform a similar observational test of the model atmospheres by using optical lines, and plotting  $\text{Ne}^{++}/\text{O}^{++}$  versus  $\text{O}^{++}/\text{O}^+$ , as shown in panel b of Figs. 6 – 9. This plot has the advantage of being independent of S/O. Figure 11 shows the observed values for a sample of Galactic H II regions (from Shaver et al. 1983, filled circles) and of Magellanic Cloud H II regions (from Pagel et al. 1978, open circles), derived using the atomic data listed in SL96. The trend seen in Fig. 11 is more compatible with the *CoStar* models than with the Kurucz ones at solar metallicity. However, it must be noted that with 0.25 solar metallicity models (more relevant to Magellanic Cloud nebulae), the problem with the Kurucz models is less severe than at solar metallicity.

It is worthwhile recalling, that, in their abundance study of low metallicity H II galaxies from optical spectroscopy, Masegosa et al. (1994) noted a completely different [Ne III] problem. Their sample showed a slight tendency for the observed  $\text{Ne}^{++}/\text{O}^{++}$  to increase as  $\text{O}^{++}/\text{O}^+$  decreases or as the  $\text{H}\beta$  equivalent width decreases. If  $\text{Ne}^{++}/\text{O}^{++}$  were to measure the abundance ratio  $\text{Ne}/\text{O}$ , this would mean that  $\text{Ne}/\text{O}$  depends on the evolutionary stage of the H II galaxy. This is of course not acceptable, and Masegosa et al. suspected that the  $\text{Ne}^{++}/\text{O}^{++}$  ratio was affected by charge exchange. Our models do take charge exchange into account. The fact that the charge transfer reaction  $\text{O}^{++} + \text{H}^0$  is far more efficient than the  $\text{Ne}^{++} + \text{H}^0$  one produces a differential effect between oxygen and neon ions, which becomes more conspicuous as the proportion of neutral hydrogen becomes greater in the  $\text{O}^{++}$  region. This is seen in our models (Figs. 6 – 9): the  $\text{Ne}^{++}/\text{O}^{++}$  ratio increases when the ionization parameter decreases. The effect found by Masegosa et al. (1994) is illustrated in Fig. 12, where we plot  $\text{Ne}^{++}/\text{O}^{++}$  versus  $\text{O}^{++}/\text{O}^+$  as derived in the sample of low metallicity H II galaxies studied by SL96 (which was based mainly on the Masegosa et al. line intensities). Because of these charge exchange reactions, it is thus difficult to test stellar model atmospheres from the diagrams shown above, if nothing is known about the ionization parameter. The only strong conclusion is that, for the Kurucz models to be consistent with the observations of nebulae with  $\text{O}^{++}/\text{O}^+ < 1$  or  $\text{O}^{++}/\text{S}^{++} < 10$ , one would require an unrealistically low ionization parameter, given the type of objects studied. On the other hand, atmosphere models including stellar winds, non-LTE effects and line blanketing naturally lead to approximately constant  $\text{Ne}^{++}/\text{O}^{++}$  values over a large domain of stellar temperatures in agreement with observations.

Another difficulty in the testing of model atmospheres by using H II regions is that many observed H II regions are in fact complexes ionized by several O stars, up to hundreds of them. The best observational test would be in fact by modelling small single-star H II regions for which

integrated line emission strengths would be available. To our knowledge, such data do not exist presently, but will be available soon (L. Deharveng, private communication).

## 6. Conclusions

We have studied the impact of modern stellar atmospheres that take into account the effects of stellar winds, departures from LTE and line blanketing on the ionization structure of H II regions. Due to a flatter energy distribution in the He I continuum, compared to the widely used Kurucz models, generally higher ionic ratios are obtained, especially for ions with high ionization potentials. For He the effect is noticeable for stellar effective temperatures below  $\sim 40000$  K.

Using the *CoStar* model predictions we find that  $\text{N}^{+}/\text{O}^+$  and  $\text{Ne}^{++}/\text{O}^{++}$  can be safely used as direct indicators of N/O and Ne/O abundance ratios, over a wide range of effective temperatures and ionization parameters.

Comparisons of observed  $\text{Ne}^{++}/\text{O}^{++}$  ionic ratios from IR line measurements and optical lines in Galactic H II regions (Shaver et al. 1983, Simpson et al. 1995) show that the *CoStar* models naturally reproduce the roughly constant observed value of  $\text{Ne}^{++}/\text{O}^{++}$ , while Kurucz models at solar metallicity fail to reproduce this behaviour. This gives a strong support to predictions of the ionizing fluxes from non-LTE atmosphere models including stellar winds and line blanketing, in agreement with the results obtained by Sellmaier et al. (1996). Compared to observations of Magellanic Cloud H II regions (Pagel et al. 1978), the low metallicity Kurucz models, however, also show a reasonable agreement.

We also point out that tests of stellar atmosphere models from observations of H II regions may be inconclusive unless one has strong constraints on the ionization parameter. Observations of integrated line strengths from single star H II regions with well known exciting sources should allow one to set much stronger constraints on the ionizing fluxes of O and B stars. This would be extremely helpful to asses the reliability of current models for O and B stars (cf. Cassinelli et al. 1995, Schaerer 1996).

*Acknowledgements.* DS acknowledges a fellowship from the Swiss National Foundation of Scientific Research and partial support from the Directors Discretionary Research Fund of the STScI.

## References

- Cassinelli J.P., Cohen D.H., MacFarlane J.J., Drew J.E., Lynas-Gray A.E., Hoare M.G., Vallerga J.V., Welsh B.Y., Vedder P.W., Hubeny I., Lanz T., 1995, ApJ 438, 932
- de Koter A., Heap S.R., Hubeny I., 1996, ApJ, in press
- de Koter A., Hubeny I., Heap S.R., Lanz T., 1994 ApJ 435, L71
- Ferland, G. J., et al. 1995, in Analysis of Emission Lines, A Meeting Honoring the 70<sup>th</sup> Birthdays of D. E. Osterbrock

- and M. J. Seaton, ed. R. E. Williams & M. Livio (Cambridge: Cambridge Univ. Press), 83
- Gabler R., Gabler A., Kudritzki R.P., Puls J., Pauldrach A., 1989, A&A 226, 162
- Kunze, D., 1994, PhD thesis, Ludwig-Maximilians Universität, Munich, Germany
- Kunze, D., Kudritzki R.P., Puls, J., 1992, in "The Atmospheres of Early Type Stars", Eds. U. Heber, C.S. Jeffery, Lecture Notes in Physics 401, Springer-Verlag, p. 45.
- Kurucz R.L., 1991, in "Stellar Atmospheres: Beyond Classical Models", NATO ASI Series C, Vol. 341, Eds. L.Crivellari, I.Hubeny, D.G.Hummer, p. 441
- Leitherer C., et al., 1996, PASP, Nov issue
- Masegosa J., Moles M., Campos-Aguilar A., 1994, ApJ 420, 576
- Mihalas D., Auer L.H., 1970, ApJ 160, 1161
- Najarro F., Kudritzki R.P., J.P. Cassinelli. O. Stahl, Hillier D.J., 1996, A&A 306, 892
- Pagel B.E.J., Edmunds M.G., Fosbury R.A.E., Webster B.L., 1978, MNRAS 184, 569
- Peimbert M., Costero R., 1969, Bol. Obs. Tonanzintla y Tacubaya 5, 3
- Rubin R.H., 1985, ApJS 57, 349
- Rubin R.H., Simpson J.P., Erickson E.F., Haas M.R., 1988, ApJ 327, 377
- Rubin R.H., Kunze D., Yamamoto T., 1995 in "Astrophysical applications of powerful New Atomic Databases, eds. Adelman S.J., and Wiese W.L., ASP Conf. Proceedings 78, p. 479
- Schaerer D., 1996, in "From Stars to Galaxies: The Impact of Stellar Physics on Galaxy Evolution", Eds. C. Leitherer, U. Fritze-von Alvensleben, J. Huchra, ASP Conf. Series 98, p. 174
- Schaerer D., de Koter A., 1996, A&A, in press (SdK96)
- Schaerer D., de Koter A., Schmutz W., Maeder A., 1996a, A&A 310, 837
- Schaerer D., de Koter A., Schmutz W., Maeder A., 1996b, A&A 312, 475
- Schaerer D., Schmutz W., 1994, A&A 288, 231
- Sellmaier F., Yamamoto T., Pauldrach A.W.A., Rubin H., 1996, A&A 305, L37 (SYPR96)
- Shaver P.A., Mc Gee R.X., Newton L.M., Danks A.C., Pottasch S.R. 1983, MNRAS 204, 53
- Simpson J.P., Colgan S.W., Rubin R.H., Erickson E.F., Haas M.R., 1995, ApJ 444, 721
- Stasińska G., 1990, A&AS 84, 501
- Stasińska G., Leitherer C., 1996, ApJS, in press (SL96)
- Vacca W.D., Garmany C.D., Shull J.M., 1996, ApJ 460, 914

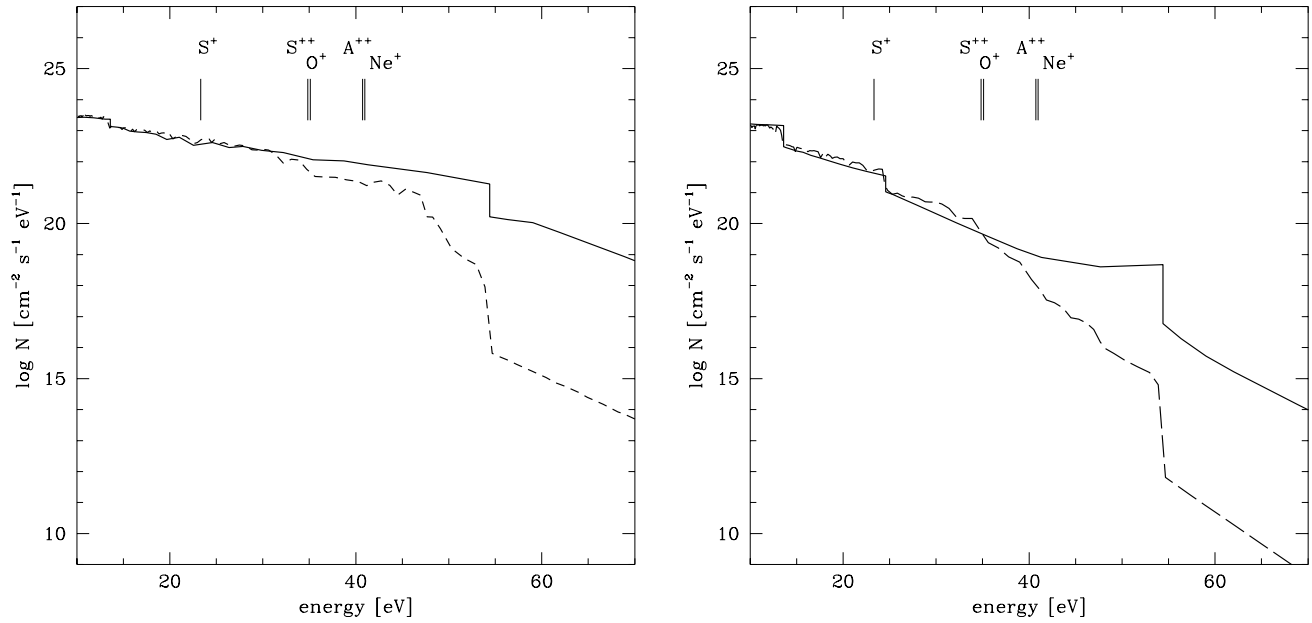


**Fig. 1.** Comparison of the EUV continuous spectral energy distribution from *CoStar* models (solid lines) and Kurucz models (dashed). Plotted is the photon number flux per unit energy as a function of the energy. Also shown are the ionization potentials of  $S^+$ ,  $S^{++}$ ,  $O^+$ ,  $Ne^+$ , and  $Ar^{++}$ . *Left panel:* *CoStar* model D2:  $(T_*, \log g) = (46.1 \text{ kK}, 4.05)$ , Kurucz:  $(T_*, \log g) = (45 \text{ kK}, 5.0)$ . *Right panel:* *CoStar* model with  $(T_*, \log g) = (35 \text{ kK}, 4.0)$  and remaining parameters from model A1, Kurucz:  $(T_*, \log g) = (35 \text{ kK}, 4.0)$

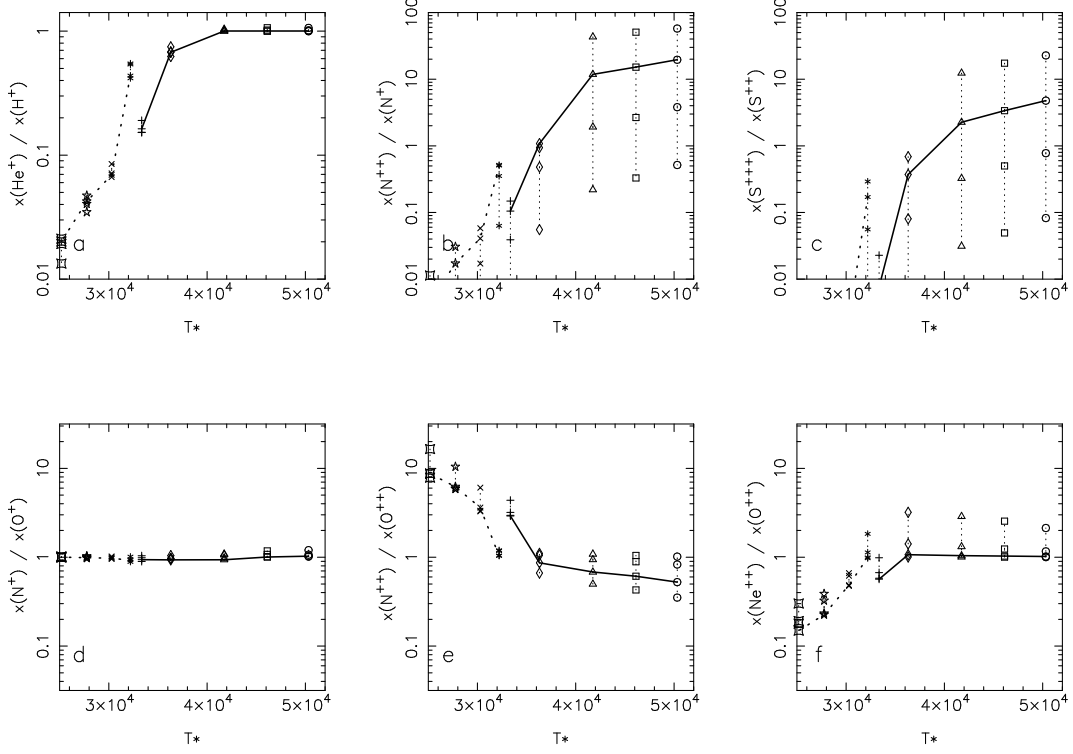


**Fig. 2.** Predicted ionic fractions  $x(X^{+n})/x(Y^{+m})$  as a function of the stellar effective temperature  $T_*$  from photoionization models using *CoStar* atmospheres at solar metallicity ( $Z=0.020$ ). At a given temperature the models 1 to 4, which differ by the ionization parameter, are connected by a thin dotted line. The “reference models” 2 are connected by the thick solid line for the main sequence stars and by the thick dotted line for giants respectively. See text for more explanations

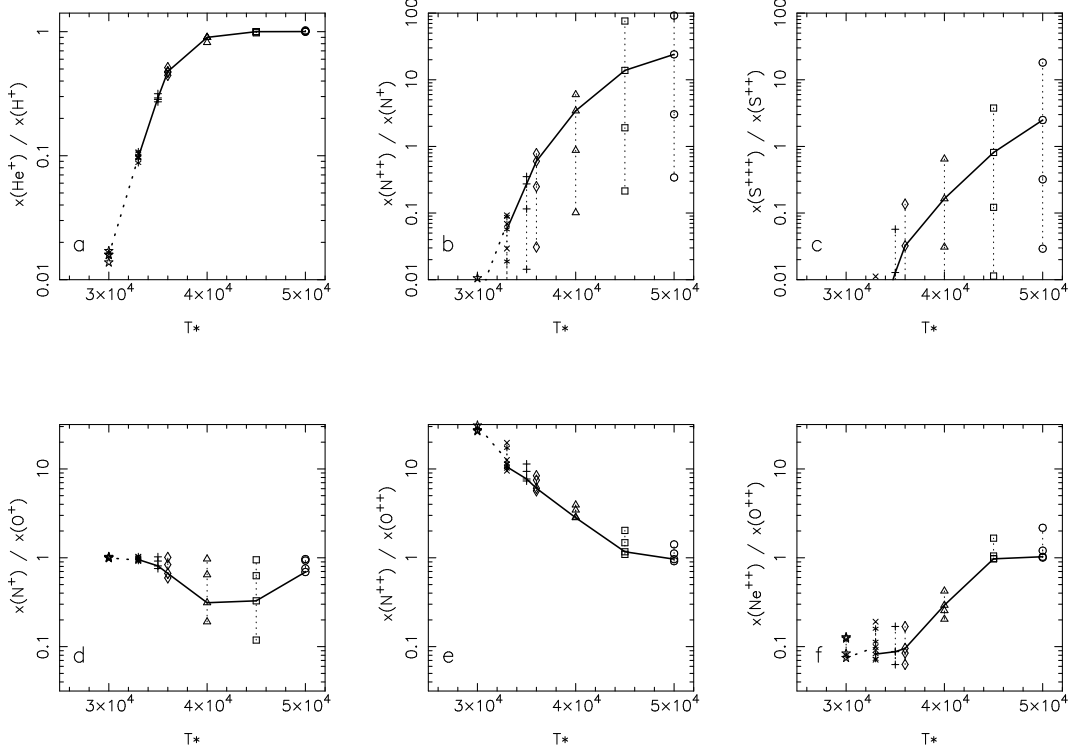


**Fig. 3.** Same as Fig. 2 for the Kurucz (1991) models at solar metallicity

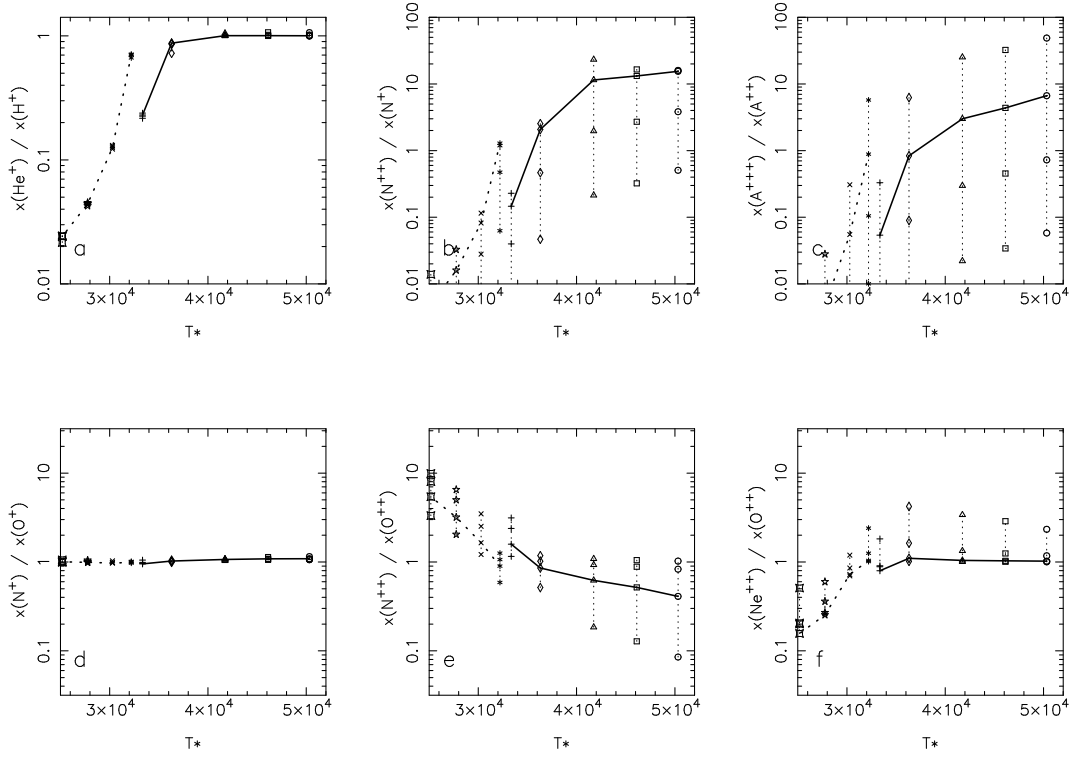


**Fig. 4.** Same as Fig. 2 for the low metallicity ( $Z=0.004$ ) *CoStar* models

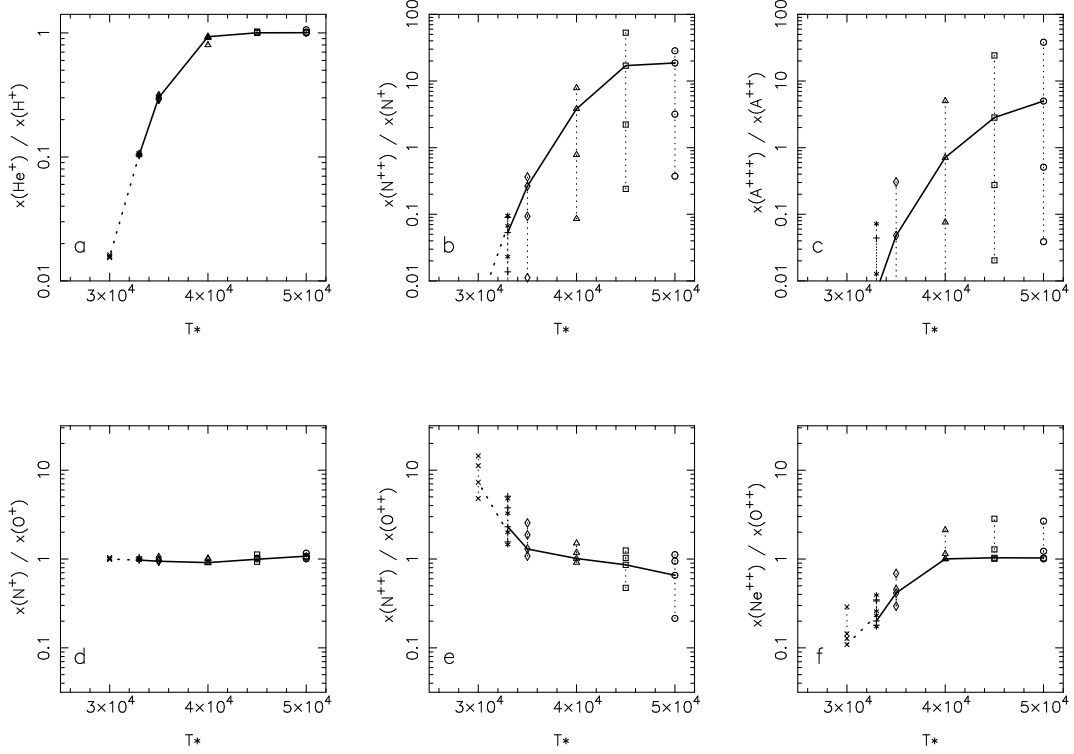


**Fig. 5.** Same as Fig. 2 for the low metallicity ( $Z=0.002$ ) Kurucz (1991) models

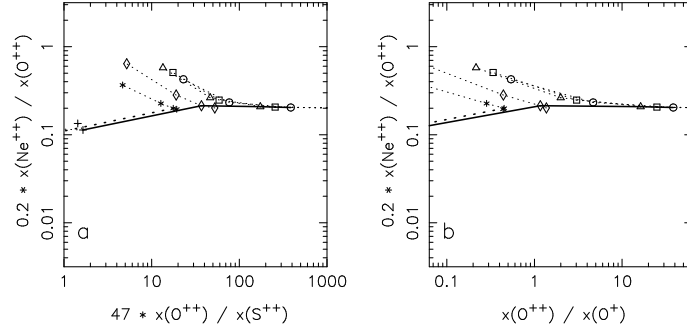


**Fig. 6.** Predicted ionic  $\text{Ne}^{++}/\text{O}^{++}$  abundance ratio as a function of the  $\text{O}^{++}/\text{S}^{++}$  ionic abundance ratio (panel a) and as a function of the  $\text{O}^{++}/\text{O}^+$  ionic fraction (panel b) for the solar metallicity *CoStar* models. Same symbols as in Fig. 2

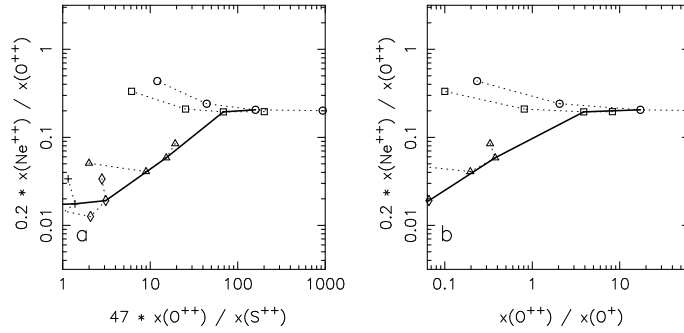


**Fig. 7.** Same as Fig. 6 for the Kurucz (1991) models at solar metallicity

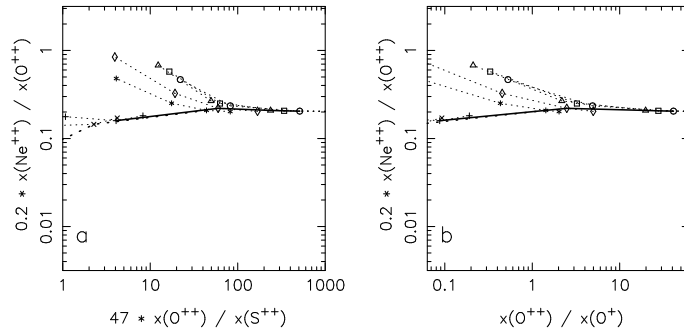


**Fig. 8.** Same as Fig. 6 for the *CoStar* models at low metallicity ( $Z=0.004$ )

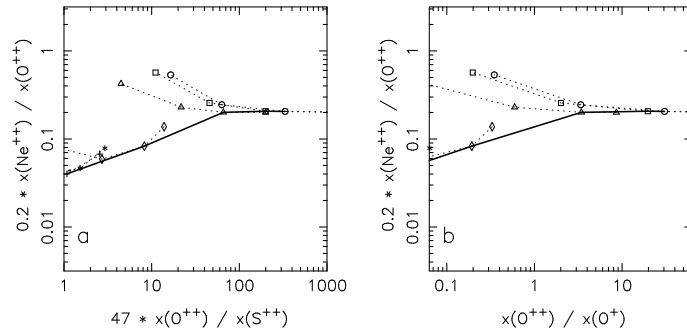


**Fig. 9.** Same as Fig. 6 for the Kurucz (1991) models at low metallicity ( $Z=0.002$ )

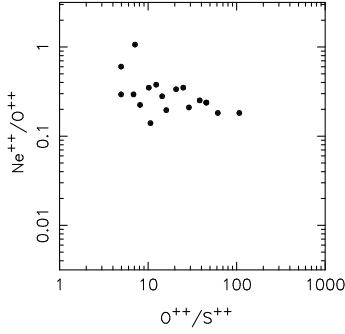


**Fig. 10.** Observed ionic  $\text{Ne}^{++}/\text{O}^{++}$  abundance ratios as a function of the  $\text{O}^{++}/\text{S}^{++}$  ionic fractions in H II regions. Data from the IR line measurements of Simpson et al. (1995). To be compared with Figs. 6a – 9 a

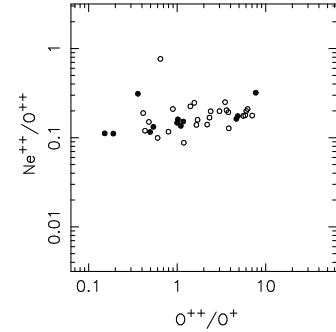


**Fig. 11.** Observed ionic  $\text{Ne}^{++}/\text{O}^{++}$  abundance ratios as a function of the  $\text{O}^{++}/\text{O}^{+}$  ionic fractions. Filled circles: Galactic H II regions, data from Shaver et al. (1983); open circles: Magellanic Cloud H II regions, data from Pagel et al. (1978). To be compared with Figs. 6b – 9 b

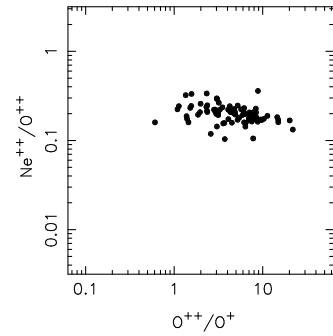


**Fig. 12.** Observed ionic  $\text{Ne}^{++}/\text{O}^{++}$  abundance ratios as a function of the  $\text{O}^{++}/\text{O}^{+}$  ionic fractions. Data from the sample of low metallicity H II galaxies studied by SL96. To be compared with Figs. 6b – 9 b